Bridge Maintenance, Safety, Management, Digitalization and Sustainability – Jensen, Frangopol & Schmidt (eds)

Challenges of implementing bridge weigh-in-motion on a century-old steel-riveted railway bridge

D. Hekič, M. Kosič, J. Kalin, A. Žnidarič & A. Anžlin
Slovenian National Building and Civil Engineering Institute, Ljubljana, Slovenia

ABSTRACT: This study explores the challenges and methodologies involved in implementing bridge weigh-in-motion (B-WIM) system on a century-old steel riveted railway bridge. A unique aspect of this study, funded by the EU H2020 Shift2Rail Joint Undertaking, was the adaptation of B-WIM systems to the specific constraints of railway bridges since, traditionally, this technology is used to collect heavy gross vehicle loading data on road bridges. The paper details the experimental setup on an old steel-riveted railway bridge, including sensor placement and calibration processes. It highlights the complexities encountered, such as differences in bridge response due to passenger and other type of trains. It introduces the system calibration strategy using known axle loads from passenger locomotives. The study provides insights into the structural response of old steel bridges under traffic loads, contributing valuable data to the field of railway bridge monitoring and maintenance.

1 INTRODUCTION

With a few exceptions (Liljencrantz et al. 2007), the bridge weigh-in-motion (B-WIM) systems have been primarily used for road bridges. The BridgeMon project (Ni Choine et al. 2014) showed that the algorithms used for road bridges can be adapted for use on railway bridges, with some constraints related to vehicle design. At the same time, B-WIM measurements within the Assets4Rail project (Anžlin et al. 2020) exposed some new challenges, likely associated with the complex behaviour of old steel bridges (Lachinger et al. 2021).

This recently concluded project, which received funding from the Shift2Rail Joint Undertaking under the EU H2020 funding, aimed to contribute to the modal shift by developing new railway asset monitoring and maintenance technologies. Part of the project was the fatigue lifetime assessment of existing steel railway bridges, considering realistic traffic loads and structural response under actual traffic loads. Performing B-WIM measurements on a century-old steel riveted bridge and under all the traffic on the bridge required some simplifications of the applied procedures. One was the B-WIM system calibration procedure, which applies axle loads and distances of statically weighed calibration vehicles as a reference. In this case, the system was calibrated using axle loads and distances of a passenger train locomotive taken from the publicly available technical specifications.

The implemented strategy worked well for random passenger trains. However, deviations have been observed when correlating the B-WIM weights of the trains with the measured displacements near the mid-span of the bridge. This paper presents the calibration procedure and monitoring results and discusses possible reasons for the load-dependent phenomena and/or challenges at B-WIM weights estimation.

2 TEST BRIDGE DESCRIPTION

The tests were performed on a 100-year-old steel-riveted bridge, shown in Figure 1. The bridge consists of two parallel steel superstructures placed on masonry abutments, spaced

DOI: 10.1201/9781003483755-167

16 m from each other and positioned obliquely to the track alignment. The distance between the structural bearings is 18.5 m. Each superstructure is 5 m wide, and the height between the rolling surface and the road below is 4.8 m. The superstructure is designed as a grillage made of steel sections connected with rivets and no welds.

Figure 1. View from the top (left) and bottom (right) of the old steel riveted bridge.

The main (plate) girders are 210 cm high and 1.2 cm thick. Its upper and bottom flange are both 25 cm wide. Close to the bridge mid-span, the thickness of the bottom flange is increased to withstand the bending moments. The 75 cm high cross girders with 32 cm width flanges distribute the load between the two main girders. The stringers (secondary longitudinal beams), placed under the railway sleepers, distribute the load to the cross girders. They are 50 cm high with 25 cm wide flanges. 1.2 cm thick steel plates are used for all stringers. The track consists of UNI 60 rails and indirect and rigid fastening systems. The wooden sleepers are anchored to the structure with metal anchor bolts.

Besides structural elements whose primary purpose is to carry vertical loads, bracing below the deck, made primarily of riveted L steel sections, carries horizontal loads. It consists of wind bracing (WB) and lateral torsional buckling bracing (LTB) of longitudinal beams.

3 EXPERIMENTAL SETUP

The bridge measurement system considered various types of sensors. The 3-axial MEMS accelerometers (DEWESoft 2023) were labelled from A01x, A01y, A01z to A12x, A12y, A12z. Four inductive strain transducers, labelled e1 to e4, measured strain in micrometres per meter (μm/m). The setup also comprised two linear variable differential transformers, LVDT1 and LVDT2, for measuring displacement. The 12 foil-type strain gauges, labelled SG01 to SG10, SMP1 and SMP2, acquire the strains in μm/m. Sensors SG01 to SG10 were used to measure the structural response, while SMP1 and SMP2 captured strains in railway rail for B-WIM axle and velocity detection purposes. The disposition of the sensors in plain view is shown in Figure 2.

After on-site inspection, the initial sensor disposition had to be adjusted as some locations were unsuitable for the sensor installation. The geometry of the entire bridge was measured on-site, and a 3D model with final sensor disposition was created (Figure 3). This model served as geometry input for creating the BIM model and integrating the sensor data in the BIM model, which was a separate test of the EU project.

Strains from the SG07 sensor installed at the midspan of the S2_L element were used to calculate the axle loads of the ongoing traffic. SG06 sensor was installed parallel to the SG07 sensor at the S2_R element. E1 sensor was installed at the midspan of the WB diagonal, which connects the CG1 and CG2 elements. SG05 was installed at the top flange of the CG4 element, and SG06 was installed at the bottom flange. SG09, SG10, and E3 sensors were mounted on the S2_L element, as shown in Figure 4.

The accelerometers A09-A12 were installed on the top flange of the PG elements, and the A01-A08 on the bottom flange. Displacements were measured with LVDT1 and LVDT2 at the left and right PG midspan, respectively. SG03 and SG04 captured strains in PG at LVDT1 and LVDT2 locations, respectively. SMP1 and SMP2 sensors were glued on the bottom side of the

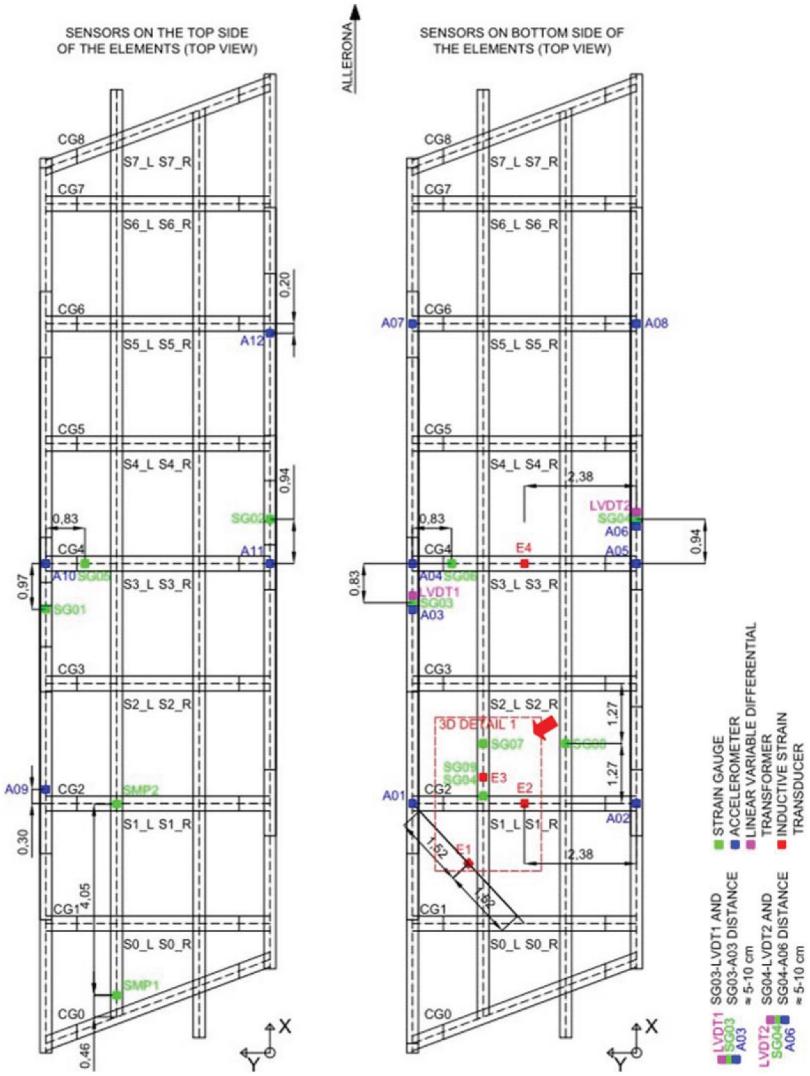

Figure 2. Disposition of the sensors in plain view on the upper (top) and lower side (bottom) of the elements.

rail to detect trains' axles and velocities for the B-WIM calculations. Finally, only SMP1 was used to detect axles. E2 and E4, installed at the midspan and the bottom flange of cross girders, provided inputs to calculate the speed of the crossing trains.

4 CALIBRATION OF THE B-WIM SYSTEM

B-WIM systems collect axle loads, axle distances and headways of all heavy freight vehicles crossing the instrumented bridge. This information is vital for optimised bridge safety analysis, which ensures structural integrity and safety of bridges and, at the same time, allows for optimal management of bridge stock. Calibration of any WIM system is essential to ensure the accuracy and reliability of measurements.

During the bridge testing, 23 train passages were recorded over 14 hours, most driving at approximately 90-100 km/h. This included seven passenger trains exhibiting similar responses and eight long freight trains. The remaining eight passages were unclassified.

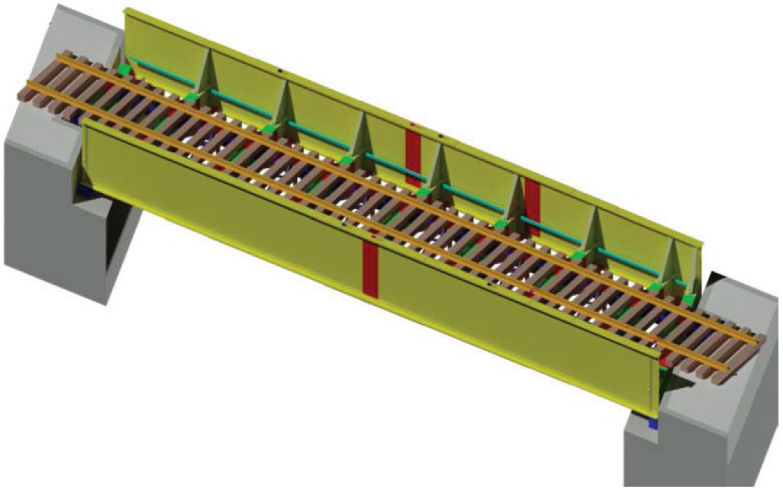

Figure 3. The 3D bridge model with sensor locations.

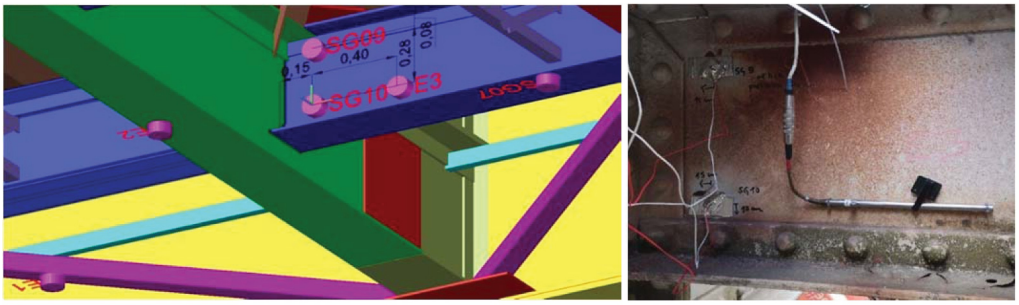

Figure 4. 3D view of the position of sensors SG07, SG09, SG10, E2, and E3 (left); installed sensors SG09, SG10 and E3 mounted on the bridge.

The B-WIM system calibration accounts for all bridge details, like concrete and steel thicknesses, which influence the relationship between the weights calculated by the B-WIM algorithm from the measured strains and the actual axle loads. For road-based B-WIM systems, calibration typically involves vehicles with statically weighed axle loads that cross the bridge multiple times. The mean value of the actual vs. measured weight ratios is taken as the calibration factor and is used to convert the strain-based results into kN.

Implementing this procedure on railway tracks is challenging as the weighing stations for trains are not always available. Furthermore, hiring a calibration train to perform multiple crossings is expensive and time-consuming. In our study, we had no information about the axle loads of the trains passing over the bridge. Nevertheless, it is beneficial for railway B-WIM applications that the weights of the locomotives are relatively consistent, especially of the electric passenger locomotives that do not carry fuel or passengers (Figure 5). The study revealed that the locomotives of these trains were of the type E.464, each with a gross weight of 72 tons (Locomotiva FS E.464. 2021).

Upon examining the signals from the B-WIM system, it was noted that the locomotives in all seven passenger train passages had almost identical axle distances and similar weights. Hence, it was assumed these were the same type of locomotives, suitable for use in calibration. The calibration factor was adjusted to align the mean Gross Vehicle Weight (GVW) of these locomotives (12 overall) to 72 tons. The standard deviation of the GVWs was 3.3% of the mean, placing the accuracy of the locomotives' GVWs in the accuracy class B(10) according to the European specifications for weigh-in-motion (Jacob et al. 2002).

Figure 5. Locomotive type E.464, captured during the test (left) and from Wikipedia (Incola 2021) (right).

5 INITIAL FE MODEL

The test bridge model was designed using the software package MIDAS Civil (2020). Its extruded 3D view is given in Figure 6.

All structural elements were formulated according to the Timoshenko beam theory, with the effect of shear deformations considered. The connections of all elements were assumed to be fixed at both ends, except for bracing elements, which were assumed to be pinned at both ends. The geometry, cross-sections and material properties were defined according to the original design documentation and on-site measurements. To model its exact geometry, rigid links were used to connect centroids of interconnected elements. While the cross-section of stringers and cross girders did not vary with length, the cross-section of the plate girder near the mid-span had more stiffening plates on the flanges. Therefore, five different cross-sections were defined only for modelling plate girders. Figure 7 compares the model with the actual structure, focusing on the cross–girder–plate detail. Rigid links were defined in the FE model to take into account the stiffening effects provided by the connection.

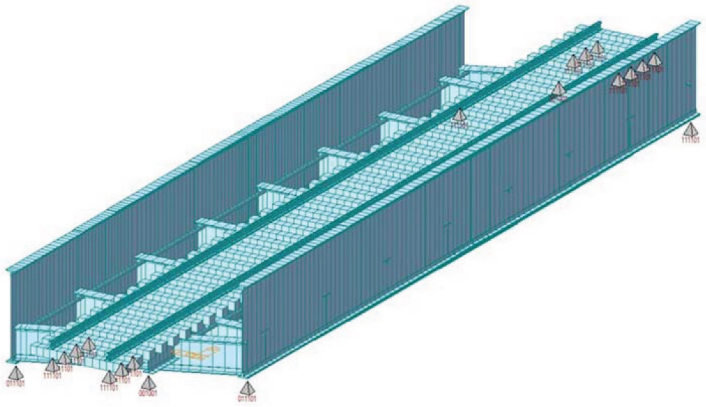

Figure 6. Extruded 3D view of the initial finite element (FE) model.

6 MANUALLY CALIBRATED FE MODEL

To more realistically estimate the remaining lifetime of the considered bridge, the initial FE model was manually calibrated to match the measured response. The calibrated FE model afterwards served to estimate the number of cycles for fatigue estimation in critical details. A series of measurements were performed for this purpose: accelerations (ambient vibrations), strains and displacements (under passing trains).

Figure 7. Cross girder – plate girder detail: structure (left) and FE model (right).

Table 1. Comparison of natural frequencies: Measurements, initial and calibrated FE model.

Frequency [Hz]	Measurements	Initial FE model	Calibrated FE model
1st bending	11.0 – 11.5	14.6	11.8
1st torsion	16.0	19.2	16.0

An enhanced frequency domain decomposition (EFDD) technique (Structural Vibration Solution 2023) was used to identify natural frequencies and mode shapes. Table 1 summarises the comparison of the measured natural frequencies with those obtained from the initial and calibrated FE model. 1st bending and 1st torsional natural frequencies were used to calibrate the FE model.

The close agreement between the measured and modelled frequencies for both bending and torsional modes was achieved mainly with additional mass, which was taken into account as a uniform increase of steel density for all steel structural elements by 11 %. This mass increase was identified by comparing the detailed 3D model (Figure 3), which included all the non-structural elements and connecting plates. While the overall mass of the initial FE model was 33 tons, the overall mass of the calibrated FE model was 37 tons (both masses exclude the mass of the sleepers and rails). Another essential modification of the initial FE model was the reduction of Young's elastic modulus of all structural elements by 5 % to globally take into account the weakened structural elements due to corrosion and loosened connections. While structural bearings, according to the design documentation, enabled the rotation of the supports both in longitudinal, transverse and vertical directions, it was observed on the site that due to corrosion of those bearings, the rotations in transverse and vertical directions might have been prevented. This was taken into account in the calibrated FE model.

Measured and modelled displacements and strains were primarily compared for passenger trains. Trains were simulated statically in the FE model, moving point forces (axles) step by step. Axle loads and distances needed to form the train in the FE model were obtained from the B-WIM.

Figure 8 compares displacements for measured response and responses of the initial and calibrated FE models during the train passage nr. 3 (passenger train). The first and last vehicles in this train were electric locomotives (Incola 2021), which were among 12 locomotives used for B-WIM calibration. GVWs of locomotives and wagons were estimated as 69.8 t, 37.1 t, 38.3 t, 36.9 t, 34.9 t, 36.7 t, 36.0 t, 37.0 t and 69.2 t. Note that although displacements capture the global response of the bridge, the number of valleys in the signals is not the same as the number of vehicles in the train. This is mainly due to the wheelbase of the wagons, which is greater than the span length.

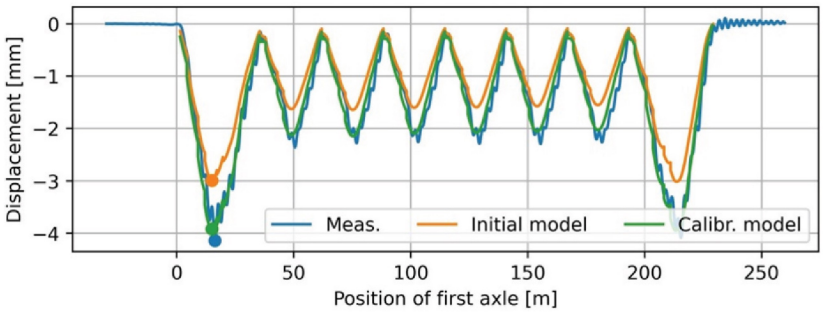

Figure 8. Comparison of measured and modelled displacements during train passage nr. 3 (passenger train) at LVDT1 sensor for the initial and manually calibrated FE model.

Comparing the FE model responses with the measurements in Figure 8, it is clear that the calibrated FE model agrees well with the actual structure. Minimum values of the measured, initial FE and calibrated FE model response are marked with blue, orange and green markers and amount to -4.1 mm, -3.0 mm and -3.9 mm, respectively.

Figure 9 compares the measured and modelled responses under the train passage nr. 9, which is a light train of unidentified type and does not contain the locomotive for B-WIM calibration. GVWs of locomotives and wagons were estimated as 49.2 t, 48.0 t and 50.3 t.

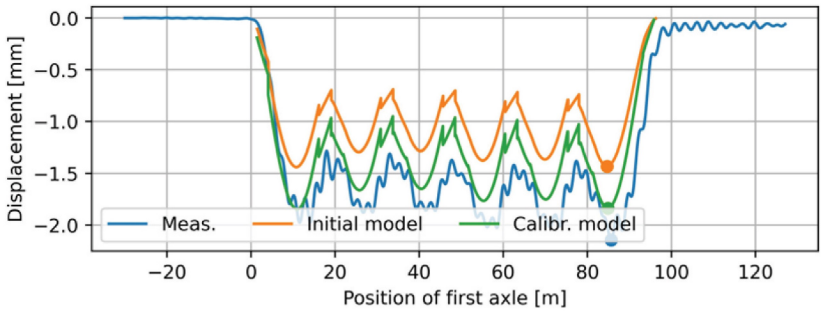

Figure 9. Comparison of measured and modelled displacements during train passage nr. 9 (light train, unidentified type) at LVDT1 sensor for the initial and manually calibrated FE model.

A comparison of the minimum measured and modelled responses of -2.1 mm, -1.4 mm and -1.8 mm (markers in Figure 9) indicates that a match of the calibrated FE model with the measurements is poorer than for the train passage nr. 3. Similar trend was observed for other train passages which are not shown in this paper, mainly for the ones which did not contain the calibration locomotives. This deviation might identify the load-dependant phenomena, such as flexibility of the connections or non-linear friction in the structural bearings. The deviation can also be viewed in the way that the weights of lighter trains were underestimated, resulting in the underestimated response of the FE model. Finally, the ratio of the mass of the calibration locomotive versus the mass of the bridge is high - approximately 2, suggesting that both the B-WIM algorithm and the FE model should be upgraded to account for the inertia effects of the passing trains, which are negligible for the roadway (concrete) bridges.

7 CONCLUSIONS

The B-WIM system application on a century-old steel-riveted railway bridge introduced challenges associated with its complex behaviour under train loading. The study demonstrated that the B-WIM system setup effectively monitored the bridge performance under the traffic

loading. The calibration procedure was adapted for railway B-WIM applications using passenger train locomotives with known and stable gross weights to calculate the calibration factors for B-WIM measurements. Those results were used to simulate the train passages in the FE model and compare the modelled and measured responses. Such a calibration process proved effective for railway B-WIM measurements but highlighted the need to extend the calibration to diverse train types.

The calibrated FE model provided an excellent match with the measured 1st bending and 1st torsional frequency. It also matched well with the measured displacements at the mid-span of the bridge, especially for the train passages that included the calibration locomotive. Deviations from the measurements were observed for trains that differed from the passage trains in terms of weights and axle configurations, indicating the possible load-dependent phenomena and/or inaccurately estimated B-WIM weights.

The results contributed to understanding the dynamic performance of old railway bridges under ambient vibrations and under train passages. Moreover, they highlighted the important contribution of the railway B-WIM systems, which provide the necessary data to calibrate the FE models on the response under train. Future research will focus on the calibration methods and explore the structural specifics and detailed modelling of various bridge designs to improve the accuracy and reliability of B-WIM measurements for railway applications. Moreover, B-WIM algorithms and the FE models should be improved to account for the dynamic response of the bridge and bridge-vehicle interaction, mostly due to large vehicle-to-bridge mass ratio.

REFERENCES

Anžlin, A., Hekič, D., Kalin, J., Kosič, M., Ralbovsky, M. & Lachinger, S. 2020. Assets4rail deliverable D3.3: Improved fatigue consumption assessment through structural and on-board monitoring.

DEWESoft, 2023. DEWESoft IOLITEi 3xMEMC-ACC [online]. Available from: https://downloads.dewesoft.com/brochures/dewesoft-iolitei-3xmems-acc-datasheet-en.pdf [Accessed 26 Dec 2023].

Incola, 2021. Locomotiva E.464.603 in sosta presso la stazione di Asti. [online]. Wikipedia. Available from: https://it.wikipedia.org/wiki/File:E.464.603_Asti.tif [Accessed 23 Sep 2021].

Jacob, B., OBrien, E.J. & Jehaes, S. (Eds.). 2002. Weigh-in-Motion of Road Vehicles: Final Report of the COST 323 Action.

Lachinger, S., Ralbovsky, M., Vorwagner, A., Hekič, D., Kosič, M. & Anžlin, A. 2021. Numerical calibration of railway bridge based on measurement data. In *Structural Engineering for Future Societal Needs; Proc. IABSE congress, Ghent 2021*: 1264–1272.

Liljencrantz, A., Karoumi, R., & Olofsson, P. 2007. Implementing bridge weigh-in-motion for railway traffic. *Computers & Structures*, 85 (1), 80–88.

Locomotiva FS E.464. [online], 2021. Wikipedia. Available from: https://it.wikipedia.org/wiki/Locomotiva_FS_E.464 [Accessed 4 Sep 2021].

MIDAS Information Technology Co., Ltd., MIDAS Civil, v1.2. [online], 2020. Available from: https://www.midasoft.com/bridge-library/civil/products/midascivil [Accessed 27 Jan 2023].

Ni Choine, M., Žnidarič, A., Corbally, R. & Kalin, J. 2014. Algorithm & Techical Specification for combined Railway Bridge WIM/SHM system.

Structural Vibration Solution. 2023. ARTeMIS Modal Pro [online]. Available from: https://www.svibs.com/artemis-modal-pro/ [Accessed 26 Dec 2023].